

Band bending and photoemission-induced surface photovoltages on clean *n*- and *p*-GaN (0001) surfaces

J. P. Long and V. M. Bermudez

Naval Research Laboratory, Washington, DC 20375-5320

(Received 8 July 2002; published 27 September 2002)

Photoelectron spectroscopy (PES) has been used to measure the dependence of core-level shifts on temperature T and source intensity for the clean (0001) surfaces of *p*- and *n*-GaN grown by metalorganic chemical vapor deposition. In the dark, the Fermi level at the surface occurs 2.55 eV above the valence band maximum for both carrier types. The surface photovoltage (SPV) induced by laboratory PES sources exceeds 1 eV on *p*-GaN at room temperature (RT). Hence PES at RT may prove impractical for determining Schottky barrier heights for optically thin metal films on *p*-GaN. The source-induced SPV falls rapidly with increasing T , persisting only to $\sim 150^\circ\text{C}$ with a standard ultraviolet PES source. This strong T dependence cannot be explained quantitatively by standard SPV models. Band bending is relatively immune to pyroelectric and piezoelectric polarization but is sensitive to chemisorbed oxygen; thermal conversion of the chemisorbed layer to an "oxide" reduces the effect of the contaminant.

DOI: 10.1103/PhysRevB.66.121308

PACS number(s): 73.30.+y, 72.40.+w, 73.61.Ey, 79.60.-i

Despite significant technological progress, much remains unknown concerning the underlying surface chemistry and physics of GaN, a wide-band-gap semiconductor ($E_G = 3.4$ eV) of interest for high-temperature and blue optoelectronic devices. An important means for investigating surface properties is photoelectron spectroscopy (PES), which measures binding energies (BE's) of electronic states near the surface. However, PES can supply misleading BE's in semiconductors¹ if the source intensity is sufficient to create a surface photovoltage (SPV). This shift in the surface electrostatic potential occurs when photoexcited electrons and holes separate in the electric field of a surface space charge layer (SCL) and hence partially screen the field² (Fig. 1). This work examines the effects of source intensity, sample temperature T , and chemisorption on SPV for *n*- and *p*-GaN. The effect of SPV on the PES of GaN, which has received little attention to date, is found to be especially significant for *p*-GaN.

Wurtzite-GaN films, ~ 2 μm thick, with Ga-polar (0001) surfaces, were grown on sapphire by metalorganic chemical vapor deposition (MOCVD). Dopants were Si ($1.6 \times 10^{17} \text{ cm}^{-3}$) for *n* type and Mg for *p* type. For *p*-GaN, after activation of Mg by annealing, Hall measurements gave 1.2×10^{17} holes cm^{-3} at room temperature (RT) from which the electrically-active Mg density (N_A) can be inferred³ by using the ionization energy I_a . Values of I_a range^{4,5} from ~ 140 to ~ 225 meV, giving N_A 's of 9×10^{17} – $2 \times 10^{19} \text{ cm}^{-3}$, which lends uncertainty both to the T -dependent bulk hole concentration and to the charge density N_{SCL} in the SCL, where N_A is essentially fully ionized.

Experiments were conducted in ultra-high vacuum (base pressure $\sim 5 \times 10^{-11}$ Torr) on surfaces cleaned by nitrogen bombardment for 10 min (1 keV, $\sim 10 \mu\text{A cm}^{-2}$) followed by a 5-min anneal at $\sim 800^\circ\text{C}$. Spectra were obtained with a double-pass cylindrical mirror analyzer. Ultraviolet photoemission spectroscopy (UPS) used a dc discharge in He, giving mainly He I ($h\nu = 21.22$ eV), the predominant flux) and He II ($h\nu = 40.81$ eV) emission. X-ray photoemis-

sion spectroscopy (XPS) was done with Mg $K\alpha$ emission at $h\nu = 1253.56$ eV. The incident photon flux was measured using the photocurrent from a sputter-cleaned Au foil with due attention to the angle of incidence ($\theta_i \approx 60^\circ$), the reflectance $R(\theta_i, h\nu)$ (computed from optical constants),⁶ and the photoelectron quantum yields.^{7,8} For GaN, $R(\theta_i, h\nu) = 0.2$ was computed⁹ for He I and taken as 0 for Mg $K\alpha$. To examine the SPV further, the near-UV flux (defined by a Corning 7-54 band-pass filter) from a 200-W high-pressure Hg-arc lamp could be focused onto the sample during PES. A 5-cm cell of deionized H_2O reduced sample heating by absorbing infrared from the Hg arc. The Hg-arc flux was measured (in air) using a pyroelectric meter and the fraction absorbed by the sample computed using GaN optical constants.¹⁰ Temperatures measured with a chromel-alumel

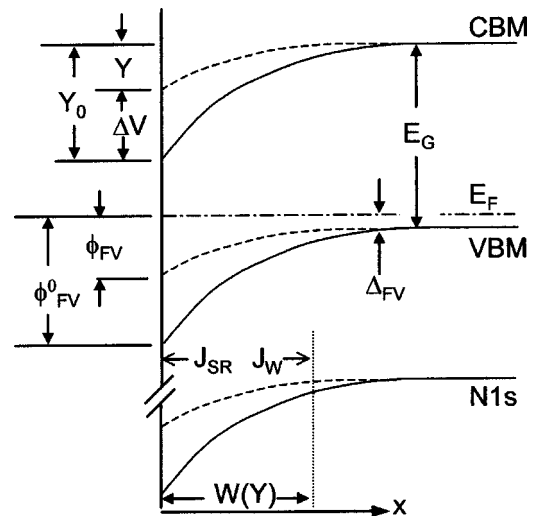


FIG. 1. Schematic diagram showing the band bending in the dark (solid lines) and under illumination (dashed lines) for *p*-GaN. The band bending Y , and shifts in Y , i.e., the SPV ΔV , are the same for the valence-band maximum (VBM) and conduction-band minimum (CBM) and for all core levels. The J 's are electron-hole current densities discussed in the text.

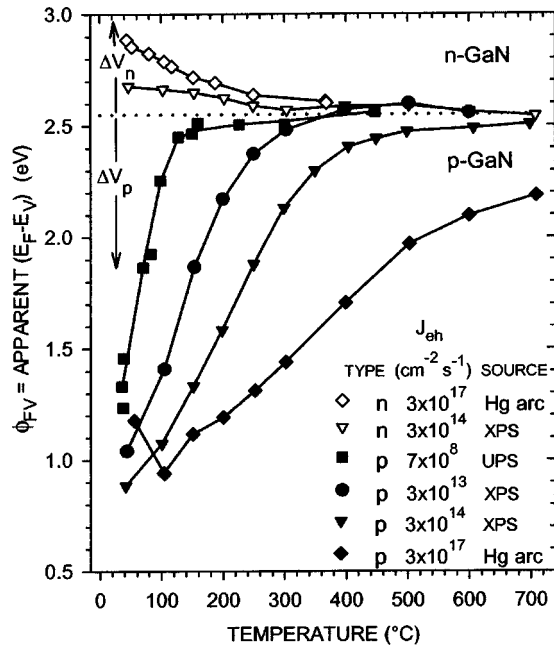


FIG. 2. ϕ_{FV} (defined in Fig. 1) vs increasing T , for n - (open symbols) and p -GaN (solid symbols). The inset gives J_{eh} , the generation rate for e - h pairs, and the PES source appropriate to each curve. “XPS” curves were obtained with different Mg-anode power levels, and “Hg arc” refers to XPS data recorded with simultaneous Hg-arc illumination. Smooth curves serve as visual aids. The dotted line at 2.55 eV gives the pinning position common to both types, and $\Delta V_{n,p}$ indicates the respective directions for increased SPV.

thermocouple pressed against the back of the sample deviated by $\leq 25^\circ\text{C}$ when checked against a pyrometer viewing a Si wafer mounted identically to the GaN. Surface cleanliness was checked after T scans (~ 6 h in duration) by XPS. Oxygen contamination was typically < 0.15 ML, compared to a saturation coverage¹¹ for chemisorption of 0.40 ML, where 1 ML is defined as one adsorbed O per surface Ga site.

Figure 2 displays the intensity and T dependence of ϕ_{FV} (cf. Fig. 1) for both n - and p -type samples as measured by XPS with and without secondary Hg-arc illumination. Also shown for p -GaN are UPS data and additional XPS data acquired with reduced x-ray flux (without Hg-arc illumination). For XPS, $\phi_{FV}(T)$ was determined from the fitted $N 1s$ kinetic energy (KE), $E_k(N 1s)$, at each T . Fitting also gave the KE of the $4d_{5/2}$ level of a grounded Au reference, and ϕ_{FV} was found from the relation $\phi_{FV} = E_B(\text{Au } 4d) + E_k(\text{Au } 4d) - E_k(N 1s) - E_V(\text{Ga } 3d) - \Delta E_{\text{Ga-N}}$. Here, $E_V(\text{Ga } 3d)$ is the BE of the Ga $3d$ relative to the valence band maximum (17.76 ± 0.03 eV, Ref. 12), $E_B(\text{Au } 4d)$ the $4d_{5/2}$ BE relative to E_F (335.22 ± 0.02 eV, Ref. 13) and $\Delta E_{\text{Ga-N}} = E_k(\text{Ga } 3d) - E_k(N 1s) = 377.5 \pm 0.1$ eV (present work). For UPS, HeII radiation was used to measure $E_k(\text{Ga } 3d)$ at each T and $\phi_{FV} = E_k(\text{Au } E_F) - E_V(\text{Ga } 3d) - E_k(\text{Ga } 3d)$ was used, where “Au E_F ” refers to the Fermi level of the Au reference.

In Fig. 2, the band bending increases with T for both doping types until ϕ_{FV} converges to a common value of $\phi_{FV}^0 = 2.55 \pm 0.15$ eV. An upward correction (< 0.3 eV) to ϕ_{FV}^0 for p -GaN may be merited if the larger values of N_A noted above pertain, in which case the attenuation length¹⁴ of

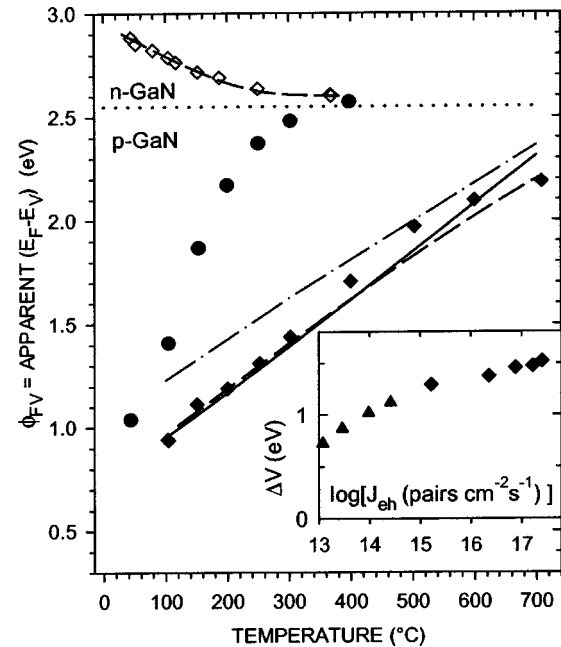


FIG. 3. Selected data from Fig. 2 (symbols correspond) and theoretical curves pertinent to Hg-arc illumination (see the text). Data for the lowest XPS flux acting alone (p -type, solid circles) illustrate the strong T dependence that cannot be reproduced by SPV models, which for low flux give slopes for ϕ_{FV} vs T that increase only slightly from those plotted. Inset: Intensity dependence of the SPV measured at 158°C by varying the XPS source flux (triangles) and at 40°C by varying secondary Hg-arc illumination via neutral density filters (diamonds). The logarithmic dependences are as expected for a SPV.

~ 1.3 nm for $N 1s$ photoelectrons is a significant fraction of the depletion depth (~ 10 nm for $N_A \sim 2 \times 10^{19} \text{ cm}^{-3}$). Our ϕ_{FV}^0 value is consistent with, but somewhat smaller than, those measured with a Kelvin probe in the dark¹⁵ for clean n - (2.94 eV) and p - (3.22 eV) GaN grown by molecular-beam epitaxy (MBE). The ϕ_{FV} convergence in Fig. 2 is attributed to the expected^{1,2,16-18} loss of SPV at elevated T . For MOCVD GaN(0001) surfaces as prepared here, the common ϕ_{FV}^0 shows that the Fermi level is essentially stationary, or pinned, against changes in doping level. If pinning is ascribed to a uniform density of surface states, $\rho_s(E)$, and if we take ϕ_{FV} for n -GaN to deviate from that of p -GaN by $\delta E < 0.2$ eV (Fig. 2), then $\rho_s(E_F) > (\sum_p - \sum_n) / \delta E \approx (0.4 \text{ to } 1) \times 10^{14} \text{ cm}^{-2} \text{ eV}^{-1}$. Here the Schottky approximation¹⁹ was used for the magnitude of the surface charge density $|\Sigma| = (2\epsilon_s q N_{\text{SCL}} |Y_0|)^{1/2}$ (charges cm^{-2}), where ϵ_s is the permittivity. A range for the lower limit to $\rho_s(E_F)$ is given because N_{SCL} depends on the uncertain value for I_a , as noted above. Given the (0001) surface atom density of $1.135 \times 10^{15} \text{ cm}^{-2}$, the estimated ρ_s indicates a highly defective surface if ρ_s arises from surface traps; intrinsic surface states in the upper part of the gap, though predicted,²⁰ have not been observed for the present samples.

Figure 3 shows that the intensity and T dependence of ϕ_{FV} are in qualitative accord with SPV models. However, the T dependence for p -GaN is much stronger than expected.^{1,16-18} The SPV can be estimated by balancing one-

dimensional generation and recombination particle-current densities, following Choo *et al.*,²¹ as

$$J_{eh}(1 - e^{-W/a}) = J_{SCL} + J_{SR} + \left[\frac{d}{\tau} \delta p - J_{eh} \frac{d}{a+d} e^{-W/a} \right], \quad (1)$$

where J_{eh} is the electron-hole pairs $\text{cm}^{-2} \text{s}^{-1}$ generated by photon absorption, W is approximately the SCL width, a is the optical absorption depth, d is the minority-carrier diffusion length, τ is the bulk recombination time, and δp is the photoexcited carrier concentration at W . The left-hand side gives the pairs $\text{cm}^{-2} \text{s}^{-1}$ photoexcited within the SCL. J_{SCL} is the pairs $\text{cm}^{-2} \text{s}^{-1}$ that recombine within the SCL, J_{SR} is the surface recombination current, and the term in brackets accounts for J_W , the diffusion current leaving (or, if negative, entering) the boundary at $x=W$. To obtain $\Delta V = Y_0 - Y$ (cf. Fig. 1), one expresses all terms in Eq. (1) as functions of Y and Y_0 , and solves for Y by iteration.²¹ In particular, δp is replaced by the solution to Poisson's equation giving Y in terms of Y_0 and δp , thereby accounting for photocarrier screening in the SCL. For our depletion layers, we use the approximation¹⁷ $\delta p = N_{SCL} (\Delta V/kT) e^{\Delta V/kT} e^{-Y_0/kT} \equiv f(Y)$, based on Ref. 22, which is valid when the quasi-Fermi-levels are flat and when $\Delta V < Y_0 - 3kT$. For a given δp , the exponentials in $f(Y)$ show why a SPV is more likely for wide-gap materials, for which the initial band bending Y_0 can greatly exceed kT .

If, in Eq. (1), one neglects J_{SCL} and the term in brackets, then Hecht's approach¹ results (Fig. 3, solid line). Alternatively, if $a \gg W$ and if $J_{SCL} + J_{SR}$ is replaced by $s \delta p$ (with s being a surface recombination velocity) then rearranging Eq. (1) recovers the solution to the steady-state diffusion equation,²¹ $\delta p = J_{eh} \tau / [(a+d)(1+s\tau/d)]$, which can then be equated to $f(Y)$ above to find ΔV (Fig. 3, dashed line). The similarity of the two limits suggests that T -dependent PES alone cannot easily distinguish the two limits. To fit the data we set $s = 2.5 \times 10^7 \text{ cm s}^{-1}$, larger than the thermal velocities of electrons and holes, which suggests a large J_{SCL} . Similarly, we had to reduce J_{eh} by a factor of 25 to obtain a fit with Hecht's approach¹ if J_{SR} included tunneling (as appropriate for $W \sim 10 \text{ nm}$), or by a factor of 500 if not. These values for s and J_{eh} are very sensitive to error in ϕ_{FV} and hence are only suggestive.

We have also performed calculations with Eq. (1), treating both simple-thermionic¹⁹ and thermionic-field^{1,19} (tunneling) models for J_{SR} , incorporating Shockley-Read-Hall recombination²¹ in J_{SCL} , allowing for electron degeneracy²³ in the SCL of p -GaN, and including³ $\Delta_{FV}(T)$. The net result for Hg-arc illumination (dot-dashed line, Fig. 3) shows no improvement in the fits and no release from the need for strong recombination. Importantly, the slopes of theoretical ϕ_{FV} vs T curves remain similar to those in Fig. 3 for all intensities, so that the strong T dependences for p -GaN cannot be reproduced. These T dependences may be due either to poorly characterized material imperfections, such as bulk and surface traps and threading dislocations that are difficult to include in an analytical SPV model, or to inadequacies in the model itself. Model limitations include use of a flat

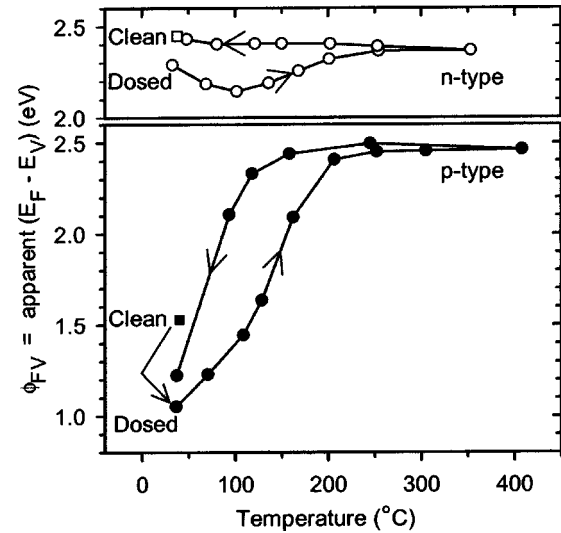


FIG. 4. UPS data for n - and p -GaN before (squares) and after (circles) a saturation exposure to O_2 near RT. Arrows show the direction of temperature change during data acquisition. The temperature-induced conversion of chemisorbed O to “oxide” at $\geq 300^\circ\text{C}$ affects the apparent SPV upon returning to lower temperature.

quasi-Fermi-level, neglect of possible photo-induced changes in surface-trap charge,^{2,17,22} and the use of a continuum approximation to treat fluxes so weak that, in the case of UPS, only one photon hits an area of πd^2 every $\sim 0.4 \text{ s}$ (for $d = 1 \mu\text{m}$).

Other factors that could influence surface electrostatics are relatively unimportant since UPS data above $\sim 150^\circ\text{C}$ exhibit a $< 0.2\text{-eV}$ further shift. These factors include a 0.4-eV shrinkage of $E_G(T)$ over our T range²⁴ and changes in polarization surface charge $\Sigma_{pol} = (\mathbf{P}_s + \mathbf{P}_p) \cdot \mathbf{n}$, where \mathbf{n} is the surface normal and \mathbf{P}_s and \mathbf{P}_p are, respectively, the spontaneous²⁵ (pyroelectric) and stress-induced (piezoelectric) polarization. \mathbf{P}_s is predicted²⁶ to produce $\sim -2 \times 10^{13} \text{ charges cm}^{-2}$ on the Ga-polar (0001) surface. As this is opposite in sign to that causing the downward band bending for p -GaN, other sources of charge on clean surfaces compensate for, or overwhelm, the effect of \mathbf{P}_s . For example, the larger of the lower limits given above for $\rho_s(E_F)$ could accommodate a charge density of this magnitude. Using the piezoelectric tensor²⁷ and the T -dependent relaxation of in-plane compressive stress,²⁸ we compute that $\mathbf{P}_p \cdot \mathbf{n}$ becomes less positive from RT to 600°C by $\sim 5 \times 10^{11} \text{ cm}^{-2}$. This change is small compared to $\Sigma_p \sim (0.6 \text{ to } 2) \times 10^{13} \text{ cm}^{-2}$ (dependent on N_{SCL}) but, because it is comparable to $-\Sigma_n \sim 1 \times 10^{12} \text{ cm}^{-2}$ that supports $Y_0 = 0.7 \text{ eV}$ on n type, it would increase Y_0 to 1.3 eV if there were no pinning mechanism.

The chemical state of the GaN surface affects the SPV. Figure 4 shows UPS data for a nominally clean surface before and after a saturation exposure to O_2 ($\sim 500 \times 10^{-6} \text{ Torr s}$). At room temperature, chemisorbed O decreases ϕ_{FV} by $\sim 0.5 \text{ eV}$ for p -GaN and $\sim 0.2 \text{ eV}$ for n -GaN. That ϕ_{FV} decreases for both types suggests that chemisorbed O causes a negative charge on the surface, the magnitude of

which (in the case of p -GaN) depends on N_{SCL} . However, at a higher synchrotron-based source flux,¹¹ chemisorbed O is observed to *increase* ϕ_{FV} for n -GaN (p -GaN not measured). This suggests that the apparent O-induced increase in ϕ_{FV} seen at higher flux is caused by the larger SPV effect which overwhelms the true decrease in ϕ_{FV} seen at a low flux. Previously¹¹ it was found that annealing a surface saturated with either chemisorbed O or H₂O at ≥ 300 °C converts chemisorbed O to an “oxide” (with O inserted into or below the surface plane) with little or no change in coverage. Figure 4 shows that this conversion causes the magnitude and T dependence of the SPV to return to nearly those of the nominally clean surface (cf. Fig. 3). Note that, for clean surfaces, the slow O contamination noted above had little effect since ϕ_{FV} routinely measured upon recooling, and during a reverse T -scan immediately after annealing, differed by ≤ 0.15 eV from results in Fig. 2.

These first quantitative PES measurements of source-

induced SPV's on GaN emphasize the need for care (especially in the case of p -doping) when interpreting BE's both for clean surfaces and for those with adsorbates or optically thin metal adlayers. While the results are specific to the Ga-polar face of wurtzite GaN grown by MOCVD, it presently appears that wurtzite p -GaN in general is prone to significant SPV-induced BE shifts. For example, large band bending has been reported¹⁵ in the dark for MBE p -type samples which, as noted above, can be expected to lead to large SPV's. In addition, a recent synchrotron UPS experiment²⁹ has also implicated SPV as the cause of temperature-dependent BE shifts for N-polar, MBE grown, p -GaN (000 $\bar{1}$).

This work was supported by the Office of Naval Research. The GaN samples were kindly supplied by R. L. Henry, D. D. Koleske, and A. E. Wickenden. J. N. Russell, Jr. is thanked for the use of the Hg-arc source. F. Bernardini is thanked for a helpful communication.

-
- ¹M. H. Hecht, Phys. Rev. B **41**, 7918 (1990).
²L. Kronik and Y. Shapira, Surf. Sci. Rep. **37**, 1 (1999).
³S. M. Sze, *Physics of Semiconductor Devices* (Wiley, New York, 1981).
⁴J. K. Sheu and G. C. Chi, J. Phys.: Condens. Matter **14**, R657 (2002).
⁵H. Wang and A.-B. Chen, Phys. Rev. B **63**, 125212 (2001).
⁶E. D. Palik, *Handbook of Optical Constants* (Academic, Orlando, FL, 1985).
⁷H. Henneken, F. Scholze, and G. Ulm, J. Appl. Phys. **87**, 257 (2000).
⁸J. A. R. Samson, *Techniques of Vacuum Ultraviolet Spectroscopy* (Pied Publications, Lincoln, NB, 1967).
⁹W. R. L. Lambrecht, B. Segall, J. Rife, W. R. Hunter, and D. K. Wickenden, Phys. Rev. B **51**, 13 516 (1995).
¹⁰T. Kawashima, H. Yoshikawa, S. Adachi, S. Fuke, and K. Ohtsuka, J. Appl. Phys. **82**, 3528 (1997).
¹¹V. M. Bermudez and J. P. Long, Surf. Sci. **450**, 98 (2000).
¹²J. R. Waldrop and R. W. Grant, Appl. Phys. Lett. **68**, 2879 (1996).
¹³C. J. Powell, Appl. Surf. Sci. **89**, 141 (1995).
¹⁴C. J. Powell and A. Jablonski, *NIST Electron Effective-Absorption-Length Database-Vers. 1* (U.S. National Institute of Standards and Technology, Gaithersburg, MD, 2001).
¹⁵M. Eyckeler, W. Mönch, T. U. Kampen, R. Dimitrov, O. Ambacher, and M. Stutzmann, J. Vac. Sci. Technol. B **16**, 2224 (1998).
¹⁶C. Bandis and B. B. Pate, Surf. Sci. **345**, L23 (1996).
¹⁷J. P. Long, H. R. Sadeghi, J. C. Rife, and M. N. Kabler, Phys. Rev. Lett. **64**, 1158 (1990).
¹⁸A. Bauer, M. Prietsch, S. Molodtsov, C. Laubschat, and G. Kaindl, Phys. Rev. B **44**, 4002 (1991).
¹⁹E. H. Roderick and R. H. Williams, *Metal-Semiconductor Contacts* (Clarendon, Oxford, 1988).
²⁰F.-H. Wang, P. Krüger, and J. Pollmann, Phys. Rev. B **64**, 035305 (2001).
²¹S. C. Choo, L. S. Tan, and K. B. Quek, Solid-State Electron **35**, 269 (1992).
²²E. O. Johnson, Phys. Rev. **111**, 153 (1958).
²³R. Seiwatz and M. Green, J. Appl. Phys. **29**, 1034 (1958).
²⁴R. Pässler, J. Appl. Phys. **90**, 3956 (2001).
²⁵F. Bernardini, V. Fiorentini, and D. Vanderbilt, Phys. Rev. B **56**, R10 024 (1997).
²⁶J. J. Harris, K. J. Lee, J. B. Webb, H. Tang, I. Harrison, L. B. Flannery, T. S. Cheng, and C. T. Foxon, Semicond. Sci. Technol. **15**, 413 (2000).
²⁷F. Bernardini and V. Fiorentini, Appl. Phys. Lett. **80**, 4145 (2002).
²⁸J. Keckes, J. W. Gerlach, R. Averbeck, H. Riechert, S. Bader, B. Hahn, H.-J. Lugauer, A. Lell, V. Härle, A. Wenzel, and B. Rauschenbach, Appl. Phys. Lett. **79**, 4307 (2001).
²⁹P. Ryan, Y.-C. Chao, J. Downes, C. McGuinness, K.E. Smith, A.V. Sampath, T.D. Moustakas, Surf. Sci. **467**, L827 (2000).